

Dissipative Dynamics of Highly Anisotropic Systems

Mauricio Martinez^{a,c}, Michael Strickland^{b,c}

^a Institut für Theoretische Physik

Goethe-Universität Frankfurt

Max-von-Laue Strasse 1

D-60438, Frankfurt am Main, Germany

^b Physics Department, Gettysburg College

Gettysburg, PA 17325 United States

^c Frankfurt Institute for Advanced Studies

Ruth-Moufang-Strasse 1

D-60438, Frankfurt am Main, Germany

Abstract

In this paper we present a method to improve the description of 0+1 dimensional boost invariant dissipative dynamics in the presence of large momentum-space anisotropies. We do this by reorganizing the canonical hydrodynamic expansion of the distribution function around a momentum-space anisotropic ansatz rather than an isotropic equilibrium one. At leading order the result obtained is two coupled ordinary differential equations for the momentum-space anisotropy and typical momentum of the degrees of freedom. We show that this framework can reproduce both the ideal hydrodynamic and free streaming limits. Additionally, we demonstrate that when linearized the differential equations reduce to 2nd order Israel-Stewart viscous hydrodynamics. Finally, we make quantitative comparisons of the evolution of the pressure anisotropy within our approach and 2nd order viscous hydrodynamics in both the strong and weak coupling limits.

Keywords: Boost Invariant Dynamics, Anisotropic Plasma, Non-equilibrium Evolution, Viscous Hydrodynamics.

1. Introduction

The remarkable success of relativistic hydrodynamics to describe the anisotropic flow of matter created during non-central heavy ion collisions [1, 2, 3, 4] has sparked a great deal interest in the systematic derivation and application of viscous hydrodynamical equations for relativistic systems [5, 6, 7, 8, 9, 10]. Here we demonstrate a method for deriving hydrodynamic-like equations for systems which have large momentum-space anisotropies. Such large momentum-space anisotropies can arise naturally due to the rapid longitudinal expansion of the matter created during relativistic heavy ion collisions. These anisotropies can become so large that the shear becomes as large as the isotropic pressure, signaling the breakdown of the expansion of the energy-momentum tensor in terms of shear corrections. In fact, in 2nd order viscous hydrodynamics large momentum-space anisotropies can even cause the longitudinal pressure predicted to become negative [11].

October 28, 2010

Here we present a way to circumvent such problems and derive evolution equations which can describe the dynamics of systems with potentially large momentum-space anisotropies. The method is to change the usual hydrodynamic expansion of the one-particle distribution functions

$$f(\tau, \mathbf{x}, \mathbf{p}) = f_{\text{eq}}(|\mathbf{p}|, T(\tau)) + \delta f_1 + \delta f_2 + \dots, \quad (1)$$

which is expansion about an isotropic equilibrium state $f_{\text{eq}}(|\mathbf{p}|, T(\tau))$, to one in which the expansion point itself can contain momentum-space anisotropies

$$f(\tau, \mathbf{x}, \mathbf{p}) = f_{\text{aniso}}(\mathbf{p}, p_{\text{hard}}(\tau), \xi(\tau)) + \delta f'_1 + \delta f'_2 + \dots, \quad (2)$$

where in both equations τ is proper time. In Eq. (2) ξ is a parameter which measures the amount of momentum-space anisotropy and p_{hard} is a non-equilibrium momentum scale which can be identified with the temperature of the system only in the limit of isotropic equilibrium. We will introduce an ansatz for f_{aniso} which approximates the system via ellipsoidal equal occupation number surfaces as opposed to the spherical ones associated with the isotropic equilibrium distribution function [12]. For highly anisotropic systems one immediately expects that the corrections $\delta f'_n$ will have smaller magnitude than the isotropic corrections δf_n due to the fact that momentum-space anisotropy is built into the leading order of the expansion in the reorganized approach. One can use different prescriptions for an anisotropic basis. Here we have in mind the use of spheroidal harmonics [13] for which our ellipsoidal ansatz is the leading order term.

Using this as a starting point, we will derive leading order 0+1 dimensional boost-invariant evolution equations for f_{aniso} by taking moments of the Boltzmann equation.¹ The result will be two coupled ordinary differential equations which describe the evolution of the system's momentum-space anisotropy and typical hard momentum scale. We demonstrate that at leading order the new expansion can equally well describe both the ideal hydrodynamic and free streaming limits within a unified framework. In addition, we demonstrate analytically that when the associated coupled nonlinear differential equations are expanded to leading order in the anisotropy parameter, they reduce identically to the 2nd order viscous hydrodynamic equations of Israel and Stewart [14, 15, 16, 17]. In the general case we solve the coupled nonlinear equations numerically allowing us to describe both the early-time high-anisotropy dynamics and late-time near-equilibrium dynamics using a single formalism which gives us as output the time-evolving distribution function. This distribution function can then be used as input for other calculations.

2. Deriving boost invariant dynamics from transport theory

We consider a highly populated system formed by massless particles. We describe this system by means of the Boltzmann equation for the one-particle distribution function $f(t, \mathbf{p}, \mathbf{x})$ in the lab frame. Additionally, we assume that the system is boost invariant and expands only along the longitudinal (beam line) axis. Boost invariance implies that

¹By leading order, we mean neglecting the corrections from the $\delta f'_n$ terms in Eq. (2).

that the longitudinal velocity of the system is constant along lines of constant spatial rapidity such that $v_z = z/t$. The assumption that the system only expands in the longitudinal direction is reliable if the transverse size of the system is sufficiently large ($\sim 1.2 A^{1/3}$ for central nucleus-nucleus collisions) that the effects of transverse dynamics can be ignored to first approximation. If this is the case then one can assume a homogeneous distribution in the transverse directions and set $v_x = v_y = 0$. With these assumptions one can show that the dynamics reduces to 0+1 dimensional evolution, i.e., only derivatives with respect to proper time remain. Here we will show how this occurs by starting in lab coordinates and transforming the Boltzmann equation to comoving coordinates. Under the assumption of homogeneity in the transverse direction one has in lab coordinates

$$p^t \partial_t f(t, z, \mathbf{p}) + p^z \partial_z f(t, z, \mathbf{p}) = -\mathcal{C}[f(t, z, \mathbf{p})], \quad (3)$$

where $\mathcal{C}[f(t, z, \mathbf{p})]$ is the collisional kernel which is a functional of the distribution function. Its functional form depends on the type of interactions between the particles and, in general, is difficult to evaluate exactly even for simple theories. To make analytic progress in this paper we will study the case that the collisional kernel is given by the relaxation time approximation

$$\mathcal{C}[f(t, z, \mathbf{p})] = p_\mu u^\mu \Gamma [f(t, z, \mathbf{p}) - f_{\text{eq}}(t, z, |\mathbf{p}|, T(\tau))], \quad (4)$$

where f_{eq} is the local equilibrium distribution function and Γ is the relaxation rate. The temperature in the local rest frame $T(\tau)$ is determined dynamically by requiring $\mathcal{E}_{\text{eq}}(\tau) = \mathcal{E}_{\text{non-eq}}(\tau)$, that guarantees energy conservation within this approximation [18] and $T(\tau)$ is assumed to only depend on the proper time $\tau = \sqrt{t^2 - z^2}$ in accordance with the assumption of boost invariance. Although here we consider the relaxation time approximation, we note that the general method can be applied to collisional kernels derived directly from quantum field theoretical methods. We postpone such studies to future publications.

2.1. Ansatz for the distribution function and equation of state

In order to have a tractable approach that will allow us to describe systems that may become highly anisotropic in momentum space we consider a general ansatz for our anisotropic distribution function which was first introduced by Romatschke and Strickland (RS) [12]. Within this approach the leading order anisotropic distribution function in the local rest frame can be obtained from an arbitrary isotropic distribution function (f_{iso}) by squeezing ($\xi > 0$) or stretching ($\xi < 0$) f_{iso} along one direction in momentum space

$$f(\tau, \mathbf{x}, \mathbf{p}) = f_{\text{RS}}(\mathbf{p}, \xi(\tau), p_{\text{hard}}(\tau)) = f_{\text{iso}}([\mathbf{p}^2 + \xi(\tau)(\mathbf{p} \cdot \hat{\mathbf{n}})^2]/p_{\text{hard}}^2(\tau)), \quad (5)$$

where p_{hard} is related to the average momentum in the partonic distribution function, $\hat{\mathbf{n}}$ is the direction of the anisotropy,² and $-1 < \xi < \infty$ is a parameter that reflects the strength and type of anisotropy. The anisotropy parameter ξ is related to the average longitudinal and transverse momentum of the constituents via the relation [19, 20]

$$\xi = \frac{\langle p_T^2 \rangle}{2\langle p_L^2 \rangle} - 1. \quad (6)$$

²Hereafter, we use $\hat{\mathbf{n}} = \hat{\mathbf{e}}_z$, where $\hat{\mathbf{e}}_z$ is a unit vector along the longitudinal direction.

The system is locally isotropic when $\xi = 0$ but this does not imply that it is in local thermal equilibrium unless f_{iso} is an equilibrium distribution function.

The energy-momentum tensor in the local rest (comoving) frame with coordinates $x^\mu = (\tau = \sqrt{t^2 - z^2}, x, y, \varsigma = \text{arctanh}(z/t))$ is given by $T^{\mu\nu} = (2\pi)^{-3} \int d^3\mathbf{p}/p^0 p^\mu p^\nu f(\tau, \mathbf{x}, \mathbf{p})$. In the comoving frame the energy-momentum tensor is diagonal and using the RS ansatz (5) its components are [21]

$$\mathcal{E}(p_{\text{hard}}, \xi) = T^{\tau\tau} = \frac{1}{2} \left(\frac{1}{1+\xi} + \frac{\arctan \sqrt{\xi}}{\sqrt{\xi}} \right) \mathcal{E}_{\text{iso}}(p_{\text{hard}}), \quad (7a)$$

$$\equiv \mathcal{R}(\xi) \mathcal{E}_{\text{iso}}(p_{\text{hard}}),$$

$$\mathcal{P}_T(p_{\text{hard}}, \xi) = \frac{1}{2} (T^{xx} + T^{yy}) = \frac{3}{2\xi} \left(\frac{1 + (\xi^2 - 1)\mathcal{R}(\xi)}{\xi + 1} \right) \mathcal{P}_{\text{iso}}(p_{\text{hard}}), \quad (7b)$$

$$\equiv \mathcal{R}_T(\xi) \mathcal{P}_{\text{iso}}(p_{\text{hard}}),$$

$$\mathcal{P}_L(p_{\text{hard}}, \xi) = -T_\varsigma^\varsigma = \frac{3}{\xi} \left(\frac{(\xi + 1)\mathcal{R}(\xi) - 1}{\xi + 1} \right) \mathcal{P}_{\text{iso}}(p_{\text{hard}}), \quad (7c)$$

$$\equiv \mathcal{R}_L(\xi) \mathcal{P}_{\text{iso}}(p_{\text{hard}}),$$

where $\mathcal{P}_{\text{iso}}(p_{\text{hard}})$ and $\mathcal{E}_{\text{iso}}(p_{\text{hard}})$ are the isotropic pressure and energy density, respectively. In general, one cannot identify immediately $\mathcal{P}_{\text{iso}}(p_{\text{hard}})$ and $\mathcal{E}_{\text{iso}}(p_{\text{hard}})$ with their equilibrium counterparts, unless one implements the Landau matching conditions [21].³ For a conformal system the tracelessness of the stress-energy tensor $T_\mu^\mu = 0$ implies $\mathcal{E} = 2\mathcal{P}_T + \mathcal{P}_L$. This condition is satisfied by Eqs. (7) for any anisotropic distribution function (5) since for an isotropic conformal state $\mathcal{E}_{\text{iso}} = 3\mathcal{P}_{\text{iso}}$.

In addition to the components of the energy-momentum tensor, one can also calculate the entropy density in the comoving frame following the standard definition from kinetic theory [23]. For the case of the RS ansatz (5) one obtains [21]

$$\begin{aligned} \mathcal{S} &= - \int \frac{d^3\mathbf{p}}{(2\pi)^3} f(\tau, \mathbf{x}, \mathbf{p}) \{ \log[f(\tau, \mathbf{x}, \mathbf{p})] - 1 \}, \\ &= \frac{\mathcal{S}_{\text{iso}}(p_{\text{hard}})}{\sqrt{1+\xi}}, \end{aligned} \quad (8)$$

where $\mathcal{S}_{\text{iso}}(p_{\text{hard}})$ is the isotropic entropy density.

An additional property of the RS ansatz (5) is that in the case of 0+1 dimensional boost invariant expansion, it is possible to relate the anisotropy parameter ξ and the shear used in viscous hydrodynamical treatments by matching the values of the longitudinal pressure \mathcal{P}_L . To see this, consider the longitudinal pressure for 0+1 dimensional viscous hydrodynamics with an ideal equation of state

$$\mathcal{P}_L(\tau) = \mathcal{P}_{\text{eq}}(T(\tau)) - \Pi(\tau) = \frac{\mathcal{E}_{\text{eq}}(T(\tau))}{3} \left(1 - \frac{3\Pi(\tau)}{\mathcal{E}_{\text{eq}}(T(\tau))} \right), \quad (9)$$

³In general the Landau matching conditions are a way to connect non-equilibrium evolution to near-equilibrium hydrodynamic evolution. In practice, this corresponds to matching the components of the energy-momentum tensor and matching collective velocities [22].

where $\Pi \equiv \Pi_\zeta^\zeta$ is the $\zeta\zeta$ component of the fluid shear tensor. The local temperature $T(\tau)$ and hard momentum scale p_{hard} contained in the RS ansatz (5) are related through the Landau matching condition for the energy density, $\mathcal{E}_{\text{eq}}(\tau) = \mathcal{E}_{\text{non-eq}}(\tau)$, which implies that at any time τ we can relate T and p_{hard} via $T = \mathcal{R}^{1/4}(\xi)p_{\text{hard}}$ [21]. By using this relation, Eq. (7c) can be rewritten as

$$\begin{aligned}\mathcal{P}_L(\tau) &= \mathcal{R}_L(\xi(\tau))\mathcal{P}_T^{\text{iso}}(p_{\text{hard}}(\tau)) = \frac{\mathcal{R}_L(\xi(\tau))}{\mathcal{R}(\xi(\tau))}\mathcal{P}_T^{\text{eq}}(T(\tau)) \\ &= \frac{\mathcal{E}_{\text{eq}}(T(\tau))}{3} \frac{\mathcal{R}_L(\xi(\tau))}{\mathcal{R}(\xi(\tau))}.\end{aligned}\quad (10)$$

Equating Eqs. (9) and (10) we find

$$\Pi(\tau) = \frac{\mathcal{E}_{\text{eq}}(T(\tau))}{3} \left[1 - \frac{\mathcal{R}_L(\xi(\tau))}{\mathcal{R}(\xi(\tau))} \right], \quad (11)$$

which is valid to all orders in ξ . In the case of small departures from equilibrium the system is very nearly isotropic with $\Pi \ll \mathcal{E}$ and one can use a small ξ expansion to obtain [21]

$$\frac{\Pi}{\mathcal{E}_{\text{eq}}} = \frac{8}{45} \xi + \mathcal{O}(\xi^2), \quad (12)$$

where \mathcal{E}_{eq} is the equilibrium energy density. If one uses the Navier-Stokes value of the shear tensor $\Pi_{\text{NS}} = 4\eta/(3\tau)$ and the ideal equation of state in the last relation, we obtain [24]

$$\xi_{\text{NS}} = \frac{10}{T\tau} \frac{\eta}{\mathcal{S}} + \mathcal{O}(\Pi_{\text{NS}}^2), \quad (13)$$

where η is the shear viscosity and \mathcal{S} is the equilibrium entropy of the system. Therefore, deviations from equilibrium which are canonically inferred from the evolution of the shear viscous tensor can be also studied using the RS distribution function (5) by analyzing the evolution of the anisotropy parameter ξ .

We point out that p_{hard} and ξ are time-dependent variables whose evolution equations are unknown a priori. In this work, we derive and solve such equations by taking the first two moments of the Boltzmann equation within the relaxation time approximation. This procedure allows us to study their time evolution and obtain information about the transition between early-time non-equilibrium dynamics and late-time viscous hydrodynamical behavior.

2.2. Boltzmann equation in comoving coordinates

It is convenient to switch to comoving coordinates

$$\begin{aligned}t &= \tau \cosh \varsigma, \\ z &= \tau \sinh \varsigma,\end{aligned}\quad (14)$$

and introduce momentum-space rapidity

$$\begin{aligned} p^0 &= p_T \cosh y, \\ p^z &= p_T \sinh y. \end{aligned} \quad (15)$$

In this coordinate system the metric $g_{\mu\nu} = \text{diag}(1, -1, -1, -\tau^2)$ and the RS ansatz (5) is $f_{\text{RS}}(\mathbf{p}, \xi, p_{\text{hard}}) = f_{\text{iso}}(p_T^2[1 + (1 + \xi) \sinh^2(y - \varsigma)]/p_{\text{hard}}^2)$. After changing variables, the Boltzmann equation (3) can be written as

$$\begin{aligned} \left(p_T \cosh(y - \varsigma) \frac{\partial}{\partial \tau} + \frac{p_T \sinh(y - \varsigma)}{\tau} \frac{\partial}{\partial \varsigma} \right) f_{\text{RS}}(\mathbf{p}, \xi, p_{\text{hard}}) = \\ -\Gamma p_T \cosh(y - \varsigma) [f_{\text{RS}}(\mathbf{p}, \xi, p_{\text{hard}}) - f_{\text{eq}}(\mathbf{p}, T(\tau))]. \end{aligned} \quad (16)$$

Note that in the above equation one should evaluate the last term on the right side using the constraint $T(\tau) = R^{1/4}(\xi)p_{\text{hard}}$ which is required by energy conservation [18, 21].

The usual way to study non-equilibrium deviations within a kinetic theory approach is to take moments of the Boltzmann equation [25]. For instance, by using the 14 moments ansatz [14, 15] it is possible to determine the equation of motion for the shear viscous tensor by taking the 2nd moment of the Boltzmann equation. In this work, we just need to determine the equations of motion for ξ and p_{hard} by considering the zeroth and first moments of the Boltzmann equation (16). We demonstrate this in the next two sections.

2.2.1. Zeroth moment of the Boltzmann equation

The zeroth moment of the Boltzmann equation with respect to the single particle energy reduces to $\partial_\mu N^\mu$ on the left hand side [23]; however, in the relaxation time approximation the zeroth moment of the collisional kernel on the right hand side is non-vanishing. Since in any realistic non-equilibrium quantum field theory there are generically number non-conserving processes we consider this to be a useful feature of the relaxation time approximation.⁴

To derive the first equation, let us first rewrite the left hand side (LHS) of Eq. (16) explicitly using the RS ansatz

$$\text{LHS} = E \partial_\omega f_{\text{RS}}(\omega) \left[\frac{p_z^2}{p_{\text{hard}}^2} \left(\partial_\tau \xi - \frac{2(1 + \xi)}{\tau} \right) - \frac{2\omega}{p_{\text{hard}}} \partial_\tau p_{\text{hard}} \right], \quad (17)$$

where $\omega \equiv [p_T^2 + (1 + \xi)p_z^2]/p_{\text{hard}}^2$ and we have rewritten the result in terms of the local energy and longitudinal momentum defined in the fluid cell via $E = p_T \cosh(y - \varsigma)$ and $p_z = p_T \sinh(y - \varsigma)$, respectively. By using this expression together with the right hand side

⁴We note that if one were considering a number-conserving theory, one can enforce $\partial_\mu N^\mu = 0$ in the relaxation time approximation by introducing a particle fugacity into the ansatz for the one particle distribution function. One would then need to take one further moment of the Boltzmann equation to determine the dynamical equations.

of Eq. (16) we can take the zeroth moment by integrating both sides with the momentum-space measure $(2\pi)^{-3} \int d^3\mathbf{p}/(2p^0)$. This results in

$$\begin{aligned} & \frac{\langle p_z^2 \partial_\omega f_{\text{RS}}(\omega) \rangle}{p_{\text{hard}}^2} \left(\partial_\tau \xi - \frac{2(1+\xi)}{\tau} \right) - \frac{2\langle \omega \partial_\omega f_{\text{RS}}(\omega) \rangle}{p_{\text{hard}}} \partial_\tau p_{\text{hard}} \\ &= -\Gamma \left[\langle f_{\text{RS}}(\mathbf{p}, \xi, p_{\text{hard}}) \rangle - \langle f_{\text{eq}}(\mathbf{p}, T(\tau)) \rangle \right] \end{aligned} \quad (18)$$

where $\langle a \rangle \equiv (2\pi)^{-3} \int d^3\mathbf{p} a(\mathbf{p})$. These integrals can be calculated analytically using the general form of the RS ansatz (5)

$$\langle p_z^2 \partial_\omega f_{\text{RS}}(\omega) \rangle = -\frac{1}{2} \frac{p_{\text{hard}}^2}{(1+\xi)^{3/2}} n_{\text{iso}}(p_{\text{hard}}), \quad (19a)$$

$$\langle \omega \partial_\omega f_{\text{RS}}(\omega) \rangle = -\frac{3}{2} \frac{n_{\text{iso}}(p_{\text{hard}})}{(1+\xi)^{1/2}}, \quad (19b)$$

$$\langle f_{\text{RS}}(\mathbf{p}, \xi, p_{\text{hard}}) \rangle = \frac{n_{\text{iso}}(p_{\text{hard}})}{(1+\xi)^{1/2}}, \quad (19c)$$

$$\langle f_{\text{eq}}(\mathbf{p}, T(\tau) = \mathcal{R}^{1/4}(\xi)p_{\text{hard}}) \rangle = \mathcal{R}^{3/4}(\xi) n_{\text{iso}}(p_{\text{hard}}), \quad (19d)$$

where in the last line we have used the Landau matching condition $T(\tau) = \mathcal{R}^{1/4}(\xi)p_{\text{hard}}$. After replacing these expressions in Eq. (18), we obtain

$$\frac{1}{1+\xi} \partial_\tau \xi - \frac{2}{\tau} - \frac{6}{p_{\text{hard}}} \partial_\tau p_{\text{hard}} = 2\Gamma \left[1 - \mathcal{R}^{3/4}(\xi) \sqrt{1+\xi} \right], \quad (20)$$

which is our first coupled differential equation for ξ and p_{hard} .

2.2.2. First moment of the Boltzmann equation

In this section we derive the second coupled differential equation for ξ and p_{hard} . Taking the first moment of the Boltzmann equation is equivalent to energy-momentum conservation $\partial_\mu T^{\mu\nu} = 0$ [23]. We enforce energy conservation by requiring that $\mathcal{E}_{\text{eq}}(\tau) = \mathcal{E}_{\text{non-eq}}(\tau)$ which results in $T(\tau) = R^{1/4}(\xi)p_{\text{hard}}$. Momentum conservation is guaranteed for any distribution function which is parity-symmetric in momentum space. In the comoving frame, energy conservation implies that the equation of motion for the energy density is

$$\frac{\partial \mathcal{E}(\tau)}{\partial \tau} = -\frac{\mathcal{E}(\tau) + \mathcal{P}_L(\tau)}{\tau}, \quad (21)$$

where \mathcal{E} and \mathcal{P}_L are the energy density and longitudinal pressure. Using the components of the energy momentum tensor given by the RS ansatz (Eqs. (7a) and (7c)) we obtain

$$\frac{\mathcal{R}'(\xi)}{\mathcal{R}(\xi)} \partial_\tau \xi + \frac{4}{p_{\text{hard}}} \partial_\tau p_{\text{hard}} = \frac{1}{\tau} \left[\frac{1}{\xi(1+\xi)\mathcal{R}(\xi)} - \frac{1}{\xi} - 1 \right], \quad (22)$$

where

$$\mathcal{R}'(\xi) = \partial_\xi \mathcal{R}(\xi) = \frac{1}{4} \left(\frac{1-\xi}{\xi(1+\xi)^2} - \frac{\arctan \sqrt{\xi}}{\xi^{3/2}} \right). \quad (23)$$

Eq. (22) is the second coupled ordinary differential equation for ξ and p_{hard} .

2.3. Combined Differential Equations

It is possible to further simplify Eqs. (20) and (22) to obtain

$$\frac{1}{1+\xi} \partial_\tau \xi = \frac{2}{\tau} - 4\Gamma \mathcal{R}(\xi) \frac{\mathcal{R}^{3/4}(\xi) \sqrt{1+\xi} - 1}{2\mathcal{R}(\xi) + 3(1+\xi)\mathcal{R}'(\xi)}, \quad (24a)$$

$$\frac{1}{1+\xi} \frac{1}{p_{\text{hard}}} \partial_\tau p_{\text{hard}} = \Gamma \mathcal{R}'(\xi) \frac{\mathcal{R}^{3/4}(\xi) \sqrt{1+\xi} - 1}{2\mathcal{R}(\xi) + 3(1+\xi)\mathcal{R}'(\xi)}. \quad (24b)$$

In the results section we show that the solution of these equations allows us to describe the transition between early-time longitudinal free streaming and late time hydrodynamical behavior. Note that one should expect that the solutions of these equations reduce to either free streaming expansion or ideal hydrodynamical behavior when $\Gamma \rightarrow 0$ or $\Gamma \rightarrow \infty$, respectively. In the next section we show this by taking the asymptotic limits of these equations.

2.4. Asymptotic limits

One way of checking self-consistency in our approach is to see if it is possible to obtain from Eqs. (24) the two extreme cases of expansion: (1) a system which undergoes 0+1 dimensional longitudinal free streaming expansion and (2) a system which is “instantaneously” thermal and isotropic and undergoes 0+1 dimensional ideal hydrodynamical expansion. In this section we show that Eqs. (24) contain both of these limits naturally.

2.4.1. Free Streaming Limit

When the particles do not interact the interaction rate Γ vanishes exactly. In order to show that the free streaming limit is recovered in our approach, we set $\Gamma = 0$ in Eqs. (24). One obtains immediately

$$\partial_\tau \xi = \frac{2}{\tau}(1+\xi), \quad (25a)$$

$$\partial_\tau p_{\text{hard}} = 0. \quad (25b)$$

The solutions of these equations are

$$\xi(\tau) = (1+\xi_0) \left(\frac{\tau}{\tau_0} \right)^2 - 1, \quad (26a)$$

$$p_{\text{hard}} = p_0, \quad (26b)$$

where ξ_0 and p_0 are the initial values of ξ and p_{hard} at $\tau = \tau_0$. This corresponds precisely to the free streaming solution to the Boltzmann equation [18, 20, 21, 26].

2.4.2. Ideal hydrodynamical expansion

In the case that the system is isotropic at all times we have $\xi(\tau) = 0$ and therefore $\partial_\tau \xi = 0$. This occurs in the limit that $\Gamma \rightarrow \infty$. From Eq. (20), we can expand the right hand side

$$\begin{aligned} \lim_{\xi \rightarrow 0} 2\Gamma \left[1 - R^{3/4}(\xi) \sqrt{1 + \xi} \right] &= 2\Gamma \left[1 - (1 + \mathcal{O}(\xi^2)) \right], \\ &= 0, \end{aligned} \quad (27)$$

so that in this limit Eq. (20) gives us

$$\frac{1}{p_{\text{hard}}} \partial_\tau p_{\text{hard}} = -\frac{1}{3\tau}. \quad (28)$$

We can also consider the same limit in Eq. (22). First, we expand the right hand side

$$\lim_{\xi \rightarrow 0} \frac{1}{\xi(1 + \xi)\mathcal{R}(\xi)} - \frac{1}{\xi} - 1 = -\frac{4}{3} + \mathcal{O}(\xi), \quad (29)$$

so that Eq. (22) reduces to

$$\frac{1}{p_{\text{hard}}} \partial_\tau p_{\text{hard}} = -\frac{1}{3\tau}. \quad (30)$$

Eqs. (28) and (30) are exactly the same and the solution is $p_{\text{hard}}(\tau) = p_{\text{hard}}(\tau_0)(\tau_0/\tau)^{1/3}$ which corresponds to the solution for the ideal 0+1 boost invariant expansion [27].⁵

2.5. Positivity of entropy divergence

One can prove analytically that the solutions to Eqs. (24) have positive entropy divergence. Formally the requirement is stated as $\partial_\mu \mathcal{S}^\mu \geq 0$ where \mathcal{S}^μ is the entropy current. In the 0+1 dimensional case this simplifies to the requirement $\partial_\tau(\tau\mathcal{S}) \geq 0$ where \mathcal{S} is the anisotropic entropy defined in Eq. (8). Using Eq. (8) we first use the chain rule to obtain

$$\frac{\partial_\tau(\tau\mathcal{S})}{\mathcal{S}} = 1 - \frac{\tau}{2(1 + \xi)} \partial_\tau \xi + \frac{3\tau}{p_{\text{hard}}} \partial_\tau p_{\text{hard}}. \quad (31)$$

Using Eqs. (24) and simplifying we find

$$\frac{\partial_\tau(\tau\mathcal{S})}{\mathcal{S}} = \tau\Gamma \left[\mathcal{R}^{3/4}(\xi) \sqrt{1 + \xi} - 1 \right]. \quad (32)$$

Since $\mathcal{R}^{3/4}(\xi) \sqrt{1 + \xi} \geq 1$ for all ξ in $-1 < \xi < \infty$ and all other quantities are positive, we therefore always have $\partial_\tau(\tau\mathcal{S}) \geq 0$. Note that in the ideal hydrodynamical limit ($\xi = 0$) and the free streaming limit ($\Gamma = 0$) the lower bound of the inequality is reached with $\partial_\tau(\tau\mathcal{S}) = 0$ as is expected.

⁵We point out that in the limit $\xi \rightarrow 0$, the local equilibrium temperature $T(\tau)$ is exactly the same as the typical momentum of the particles in the system p_{hard} since $\mathcal{R}(0) = 1$.

2.6. 2nd order viscous hydrodynamics from RS ansatz

In Sect. 2.1 we showed that in the near-equilibrium limit one can relate the viscous shear tensor Π with the anisotropy parameter ξ (Eq. (12)). As a consequence, in our approach, the evolution of dissipative corrections to the ideal fluid is equivalent to the evolution of the anisotropy parameter ξ . To see this more in detail, in this section we derive the equations of motion for 2nd order 0+1 boost invariant viscous hydrodynamics from the RS ansatz (5) by linearizing the previously obtained coupled nonlinear differential equations.

We begin by using Eq. (21) for the energy density, Eq. (10) for the matching between ξ and Π , and assume an ideal equation of state.⁶ The result is

$$\partial_\tau \mathcal{E} = -\frac{\mathcal{E}}{\tau} \left(1 + \frac{\mathcal{R}_L(\xi)}{3\mathcal{R}(\xi)} \right), \quad (33)$$

which upon using (11) gives

$$\partial_\tau \mathcal{E} = -\frac{\mathcal{E} + \mathcal{P}}{\tau} + \frac{\Pi}{\tau}. \quad (34)$$

This expression is the well-known equation for the energy density when the system has shear viscous corrections in a 0+1 dimensional boost-invariant expansion [14, 15, 16].

To obtain the equation of motion for the shear viscous tensor we use Eq. (20) derived in Sect. 2.2.1. First, let us rewrite some terms which appear in this equation by using the linear relation between ξ and Π

$$\partial_\tau \xi = \frac{45}{8} \left(\frac{\partial_\tau \Pi}{\mathcal{E}} - \frac{\Pi}{\mathcal{E}} \frac{\partial_\tau \mathcal{E}}{\mathcal{E}} \right), \quad (35)$$

where \mathcal{E} is understood to be the isotropic equilibrium energy density in this section. Next, by implementing the Landau matching condition for the local temperature and p_{hard} we obtain

$$\frac{\partial_\tau p_{\text{hard}}}{p_{\text{hard}}} = \frac{1}{4} \left(\frac{\partial_\tau \mathcal{E}}{\mathcal{E}} - \frac{\mathcal{R}'(\xi)}{\mathcal{R}(\xi)} \partial_\tau \xi \right). \quad (36)$$

Plugging the last two expressions into Eq. (20), using Eqs. (12) and (34), and expanding to the lowest non-vanishing order in ξ one obtains

$$\partial_\tau \Pi + \frac{4}{3} \frac{\Pi}{\tau} - \frac{16}{45} \frac{\mathcal{E}}{\tau} = -\frac{1}{2} \Gamma \Pi. \quad (37)$$

To finally connect with second order viscous hydro, we identify⁷

$$\Gamma = \frac{2}{\tau_\pi}, \quad (38a)$$

$$\tau_\pi = \frac{5}{4} \frac{\eta}{\mathcal{P}}, \quad (38b)$$

⁶During the derivation presented in this section, it is necessary to implement the Landau matching condition which relates the local temperature and the average momentum of the particles p_{hard} , i.e. $T(\tau) = \mathcal{R}^{1/4}(\xi(\tau))p_{\text{hard}}(\tau)$.

⁷This is analogous to the identifications of the unknown coefficients β_0 , β_1 and β_2 which appear in the 14 Grad's ansatz [14, 15, 16, 17, 28, 29].

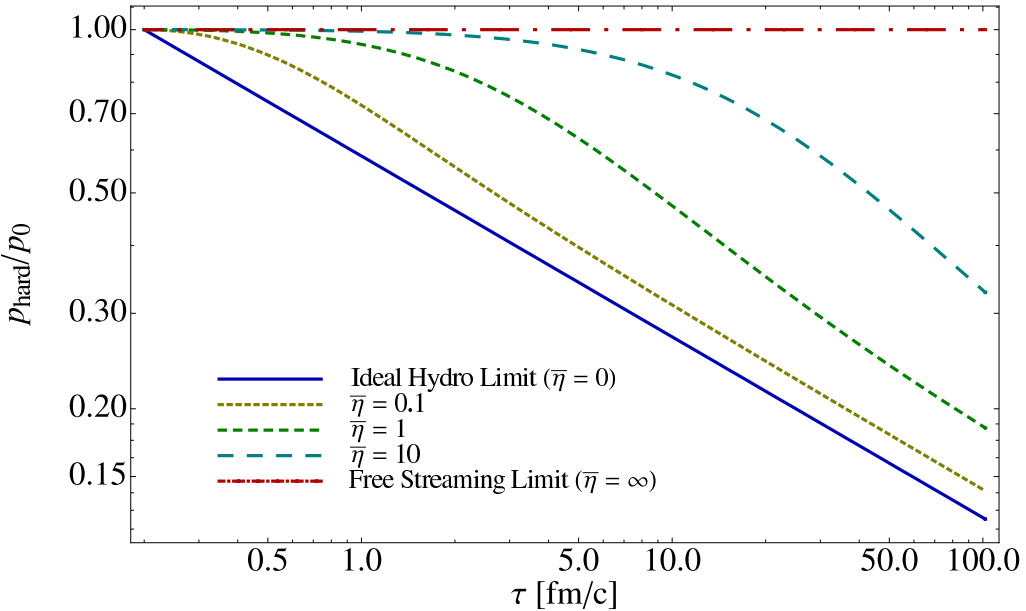


Figure 1: Hard momentum scale p_{hard} as a function of proper time for five different values of $\bar{\eta}$: the ideal hydrodynamic limit ($\bar{\eta} = 0$), $\bar{\eta} = 0.1$, $\bar{\eta} = 1$, $\bar{\eta} = 10$, and the free streaming limit ($\bar{\eta} = \infty$).

so Eq. (37) can be written finally as

$$\partial_\tau \Pi = -\frac{\Pi}{\tau_\pi} + \frac{4}{3} \frac{\eta}{\tau_\pi \tau} - \frac{4}{3} \frac{\Pi}{\tau}, \quad (39)$$

where τ_π and η are the shear relaxation time and shear viscosity, respectively. This last expression is precisely the 0+1 dimensional 2nd order viscous hydrodynamical equation for Π [14, 15, 16]. Therefore, the physics of 2nd order viscous hydrodynamics can be recovered from our ansatz in the small ξ limit.

3. Results

In this section we present the results of numerically integrating the coupled nonlinear differential equations using the relation between the relaxation rate Γ and the ratio of shear viscosity to equilibrium entropy $\bar{\eta} \equiv \eta/\mathcal{S}$ which results from Eqs. (38), namely

$$\Gamma = \frac{2T(\tau)}{5\bar{\eta}} = \frac{2\mathcal{R}^{1/4}(\xi)p_{\text{hard}}}{5\bar{\eta}}, \quad (40)$$

which should be used for Γ in Eqs. (24). In all plots shown in this paper we will use the following initial conditions: $\tau_0 = 0.2$ fm/c, $p_{\text{hard}}(\tau = \tau_0) = 350$ MeV, and $\xi(\tau = \tau_0) = 0$. Note, however, that one can choose whatever initial conditions one likes in order to integrate Eqs. (24).

In Fig. 1 we show the solutions obtained for the hard momentum scale p_{hard} as a function of proper time for five different values of $\bar{\eta}$: the ideal hydrodynamic limit ($\bar{\eta} = 0$), $\bar{\eta} = 0.1$,

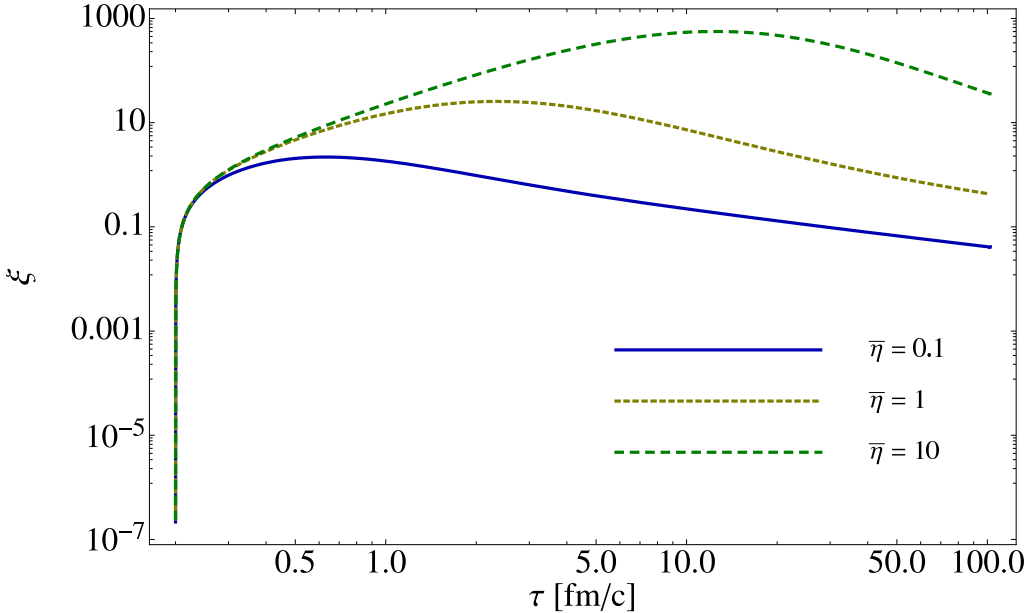


Figure 2: Anisotropy parameter ξ as a function of proper time for three different values of $\bar{\eta}$: $\bar{\eta} = 0.1$, $\bar{\eta} = 1$, and $\bar{\eta} = 10$.

$\bar{\eta} = 1$, $\bar{\eta} = 10$, and the free streaming limit ($\bar{\eta} = \infty$). As can be seen from this figure, the solutions to Eqs. (24) make a smooth transition from ideal hydrodynamic behavior to longitudinal free streaming as $\bar{\eta}$ goes from 0 to ∞ . For finite values of $\bar{\eta}$ one sees that the solutions smoothly transition between early-time longitudinal free streaming and late-time viscous hydrodynamical behavior.

In Fig. 2 we show the corresponding solutions for the anisotropy parameter ξ as a function of proper time for three different values of $\bar{\eta}$: $\bar{\eta} = 0.1$, $\bar{\eta} = 1$, and $\bar{\eta} = 10$. In the ideal hydrodynamic limit one has $\xi = 0$ and in the free streaming limit one has $\xi = (1 + \xi_0)(\tau/\tau_0)^2 - 1$. The solutions presented in Fig. 2 show that at very early times the behavior of the system only depends weakly on $\bar{\eta}$ due to the rapid longitudinal expansion of the system. In addition, in all cases, the anisotropy has a maximum which is obtained at later proper times as $\bar{\eta}$ is increased.

Knowledge of the proper-time dependence of p_{hard} and ξ allows one to calculate all of the various thermodynamic functions defined in Eqs. (7a), (7b), (7c), and (8). For sake of brevity we do not show each of these individually but we note that the energy density smoothly transitions from early-time free streaming to late-time hydrodynamical expansion as one would expect. A quantity that is sensitive to momentum-space anisotropies is the ratio of the longitudinal to transverse pressures, $\mathcal{P}_L/\mathcal{P}_T$. In the ideal hydrodynamic limit this is identically one and in the free streaming limit one obtains $\mathcal{P}_L/\mathcal{P}_T \propto 1/\tau^2$ at late times. In Fig. 3 we show $\mathcal{P}_L/\mathcal{P}_T$ for three different values of $\bar{\eta}$: $\bar{\eta} = 0.1$, $\bar{\eta} = 1$, and $\bar{\eta} = 10$. One sees from this figure that as $\bar{\eta}$ is increased, the longitudinal pressure is decreased; however, at late times the system restores isotropy in momentum space for any finite $\bar{\eta}$. It is important to note that even for the case $\bar{\eta} = 10$ the longitudinal pressure of the system remains positive

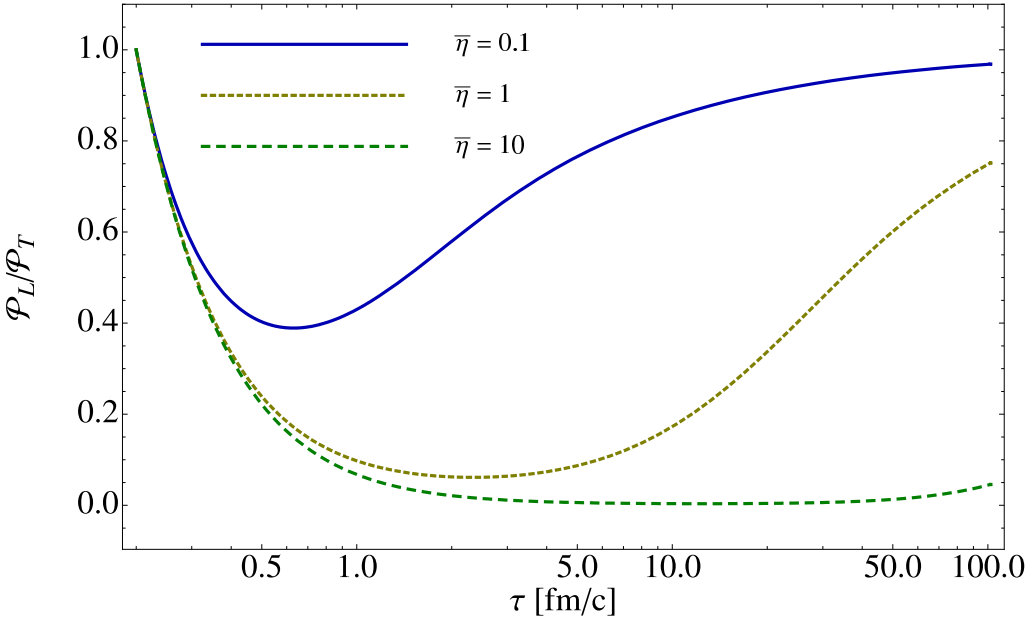


Figure 3: Ratio of longitudinal [Eq. (7c)] and transverse [Eq. (7b)] pressures as a function of proper time for three different values of $\bar{\eta}$: $\bar{\eta} = 0.1$, $\bar{\eta} = 1$, and $\bar{\eta} = 10$.

definite.

Having obtained the general numerical solutions to Eqs. (24) we can now make a quantitative comparison between solution to the fully nonlinear differential equations (24) and the linearized 2nd order viscous hydrodynamical equations given by Eqs. (34) and (39). In Figs. 4 and 5 we compare the two approaches for typical strong and weak coupling values of $\bar{\eta} = 1/(4\pi)$ and $\bar{\eta} = 10/(4\pi)$, respectively. As one can see from Fig. 4 for $\bar{\eta} = 1/(4\pi)$ the difference between the RS ansatz solutions and 2nd order viscous hydro is at maximum approximately 15%. However, in the weak coupling case of $\bar{\eta} = 10/(4\pi)$ one finds that the correction can be greater than 100%. More importantly, one finds that in the weak coupling case, for the chosen initial conditions, the ratio $\mathcal{P}_L/\mathcal{P}_T$ obtained from 2nd order viscous hydrodynamics becomes negative for $0.65 \text{ fm}/c \lesssim \tau \lesssim 5.9 \text{ fm}/c$ whereas the solution obtained using the RS ansatz is positive definite during the entire evolution. Quantitatively one should note that even in the strong coupling case large momentum-space anisotropies can be developed with $\min(\mathcal{P}_L/\mathcal{P}_T) \sim 0.45$ even for the exact solution. The precise numbers, of course, depend on the choice of the initial conditions and proper time at which one begins integrating the differential equations. When cast into dimensionless form the relevant quantity is $\tau_0 T$ with larger values of the dimensionless number corresponding to generation of smaller momentum-space anisotropies.

4. Conclusions and Outlook

In this paper we have shown that by starting from an ansatz which incorporates momentum-space anisotropies from the beginning one can obtain solutions which smoothly connect the

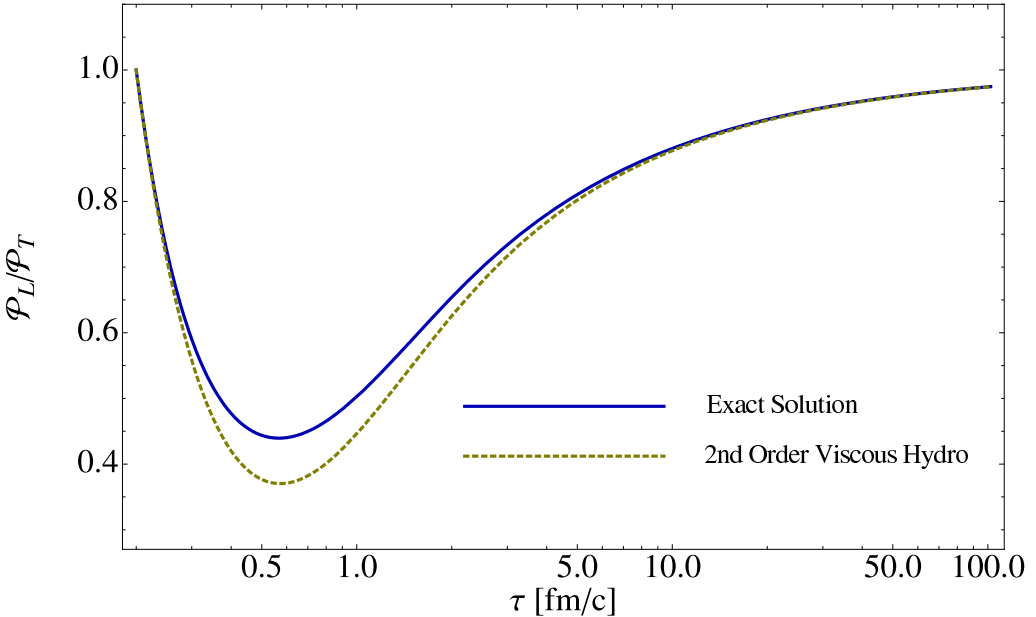


Figure 4: Ratio of longitudinal [Eq. (7c)] and transverse [Eq. (7b)] pressures as a function of proper time for $\bar{\eta} = 1/(4\pi)$. Solid line is numerical solution to Eqs. (24) and dashed line is numerical solution of 2nd order viscous hydrodynamics given by equations (34) and (39).

ideal hydrodynamic and free streaming limits by varying $\bar{\eta}$ from zero to infinity. We demonstrated that these limits are achieved analytically and numerically. In addition, we showed that when the equations are linearized the resulting linear differential equations reduce to the Israel-Stewart equations for viscous hydrodynamical evolution. We then made a detailed comparison of the prediction for the ratio of longitudinal to transverse pressure predicted by the RS ansatz and the Israel-Stewart formalism. We found that for typical strong coupling values of $\bar{\eta}$ the correction from 2nd order viscous hydrodynamical evolution was on the order of 15% and for a typical weak coupling value of $\bar{\eta}$ that the correction was sizable and could be greater than 100%.

The conclusions reached here are based on one particular set of initial conditions, however, the pattern observed here is generic. At LHC energies the initial time of hydro evolution is expected to be less based on perturbative estimates of the thermalization time; however, the initial temperature is also expected to be higher. When cast into dimensionless form what matters is the dimensionless combination $\tau_0 T_0$ for determining the magnitude of expected longitudinal momentum-space anisotropies. For the RHIC-like initial conditions presented here this combination is $\tau_0 T_0 = 0.35$ whereas for LHC-like initial conditions one obtains $\tau_0 T_0 = 0.43$ assuming $\tau_0 = 0.1$ fm/c and $T_0 = 850$ MeV. Therefore, one expects slightly smaller momentum-space anisotropies to be generated for LHC initial conditions.

The method shown here can be used as input to calculate the dependence of high energy observables on the time evolution of the anisotropy parameter and hard momentum scale. There are now calculations of the anisotropic photon rate [30], dilepton rate [19, 20, 31], and quarkonium binding energies [32, 33, 34] using the RS ansatz. It would be interesting

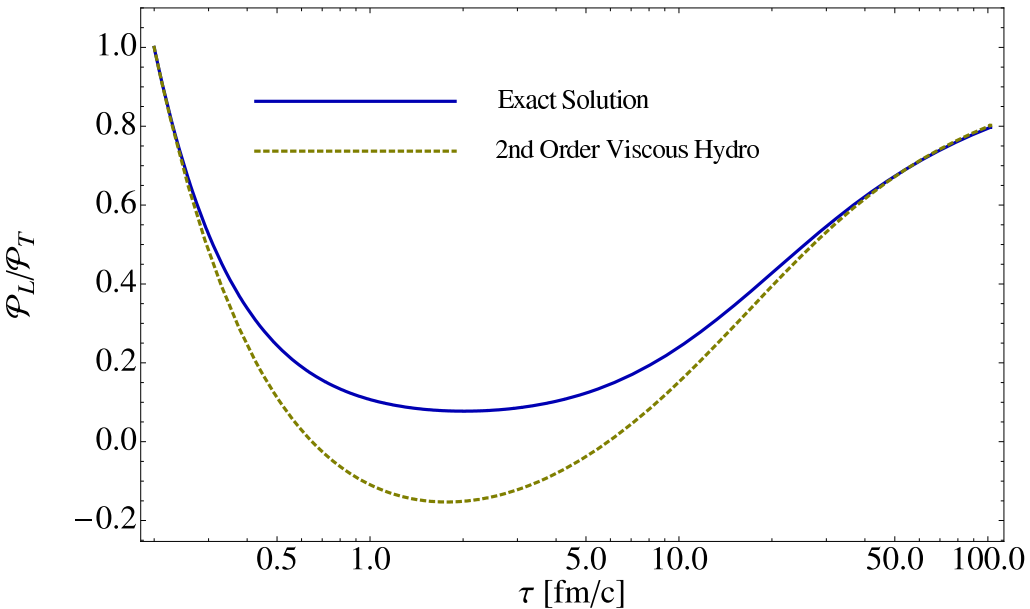


Figure 5: Ratio of longitudinal [Eq. (7c)] and transverse [Eq. (7b)] pressures as a function of proper time for $\bar{\eta} = 10/(4\pi)$. Solid line is numerical solution to Eqs. (24) and dashed line is numerical solution of 2nd order viscous hydrodynamics given by equations (34) and (39).

to apply the differential equations derived here to these phenomenological applications.

In addition, looking forward one can also extend the ansatz used here to allow for the inclusion of particle fugacities. This can be done by evaluating another moment of the Boltzmann equation; however, one will need to take care with the time evolution of the number density in this case if one wants to obtain solutions which reach chemical equilibrium at late times [35]. We postpone this development to a future paper.

Note Added

During the final preparation of this manuscript another paper presenting a similar idea appeared by Florkowski and Ryblewski [36]. However, they obtain two differential equations by requiring energy conservation and introducing an ansatz for an entropy source whereas we follow the method of taking moments of the Boltzmann equation directly.

Acknowledgments

We thank A. El, G. Denicol, A. Dumitru, C. Greiner, P. Huovinen, H. Niemi, P. Romatschke, A. Rebhan, and Z. Xu for useful discussions. M. Martinez and M. Strickland were supported by the Helmholtz International Center for FAIR Landesoffensive zur Entwicklung Wissenschaftlich-Ökonomischer Exzellenz program.

References

- [1] P. Huovinen, P. F. Kolb, U. W. Heinz, P. V. Ruuskanen, and S. A. Voloshin, “Radial and elliptic flow at RHIC: further predictions,” *Phys. Lett.* **B503** (2001) 58–64, arXiv:hep-ph/0101136.

- [2] T. Hirano and K. Tsuda, “Collective flow and two pion correlations from a relativistic hydrodynamic model with early chemical freeze out,” *Phys. Rev.* **C66** (2002) 054905, arXiv:nucl-th/0205043.
- [3] M. J. Tannenbaum, “Recent results in relativistic heavy ion collisions: From ‘a new state of matter’ to ‘the perfect fluid’,” *Rept. Prog. Phys.* **69** (2006) 2005–2060, arXiv:nucl-ex/0603003.
- [4] P. F. Kolb and U. W. Heinz, “Hydrodynamic description of ultrarelativistic heavy-ion collisions,” arXiv:nucl-th/0305084.
- [5] K. Dusling and D. Teaney, “Simulating elliptic flow with viscous hydrodynamics,” *Phys. Rev.* **C77** (2008) 034905, arXiv:0710.5932 [nucl-th].
- [6] M. Luzum and P. Romatschke, “Conformal Relativistic Viscous Hydrodynamics: Applications to RHIC results at $\sqrt{s_{NN}} = 200$ GeV,” *Phys. Rev.* **C78** (2008) 034915, arXiv:0804.4015 [nucl-th].
- [7] H. Song and U. W. Heinz, “Extracting the QGP viscosity from RHIC data – a status report from viscous hydrodynamics,” arXiv:0812.4274 [nucl-th].
- [8] U. W. Heinz, “Early collective expansion: Relativistic hydrodynamics and the transport properties of QCD matter,” arXiv:0901.4355 [nucl-th].
- [9] J. Peralta-Ramos and E. Calzetta, “Divergence-type nonlinear conformal hydrodynamics,” *Phys. Rev.* **D80** (2009) 126002, arXiv:0908.2646 [hep-ph].
- [10] J. Peralta-Ramos and E. Calzetta, “Divergence-type 2+1 dissipative hydrodynamics applied to heavy-ion collisions,” arXiv:1003.1091 [hep-ph].
- [11] M. Martinez and M. Strickland, “Constraining relativistic viscous hydrodynamical evolution,” *Phys. Rev.* **C79** (2009) 044903, arXiv:0902.3834 [hep-ph].
- [12] P. Romatschke and M. Strickland, “Collective Modes of an Anisotropic Quark-Gluon Plasma,” *Phys. Rev.* **D68** (2003) 036004.
- [13] M. Abramowitz and I. A. Stegun, “Spheroidal wave functions,” in *Handbook of Mathematical Functions with Formulas, Graphs, and Mathematical Tables*, pp. 751–770. Dover, New York, 1964.
- [14] W. Israel, “Nonstationary irreversible thermodynamics: A Causal relativistic theory,” *Ann. Phys.* **100** (1976) 310–331.
- [15] W. Israel and J. M. Stewart, “Transient relativistic thermodynamics and kinetic theory,” *Ann. Phys.* **118** (1979) 341–372.
- [16] A. Muronga, “Second order dissipative fluid dynamics for ultra- relativistic nuclear collisions,” *Phys. Rev. Lett.* **88** (2002) 062302, arXiv:nucl-th/0104064.
- [17] A. Muronga, “Causal Theories of Dissipative Relativistic Fluid Dynamics for Nuclear Collisions,” *Phys. Rev.* **C69** (2004) 034903, arXiv:nucl-th/0309055.
- [18] G. Baym, “Thermal equilibration in Ultrarelativistic Heavy Ion Collisions,” *Phys. Lett.* **B138** (1984) 18–22.
- [19] M. Martinez and M. Strickland, “Measuring QGP thermalization time with dileptons,” *Phys. Rev. Lett.* **100** (2008) 102301.
- [20] M. Martinez and M. Strickland, “Pre-equilibrium dilepton production from an anisotropic quark-gluon plasma,” *Phys. Rev.* **C78** (2008) 034917.
- [21] M. Martinez and M. Strickland, “Matching pre-equilibrium dynamics and viscous hydrodynamics,” *Phys. Rev.* **C81** (2010) 024906.
- [22] L. Landau and E. Lifschitz, *Fluid mechanics*. Course of theoretical physics / by L.D. Landau and E.M. Lifshitz, Vol. 6. Butterworth-Heinemann, 2 ed., 1987.
- [23] S. R. de Groot, W. A. van Leewen, and C. G. van Weert, *Relativistic Kinetic Theory: principles and applications*. Elsevier North-Holland, 1980.
- [24] M. Asakawa, S. A. Bass, and B. Muller, “Anomalous transport processes in anisotropically expanding quark-gluon plasmas,” *Prog. Theor. Phys.* **116** (2007) 725–755.
- [25] H. Grad, “On the kinetic theory of rarefied gases,” *Commun. Pure Appl. Math.* **2** (1949) 331.
- [26] J. I. Kapusta, L. D. McLerran, and D. Kumar Srivastava, “Rates for dilepton production at RHIC and LHC between J / psi and upsilon are big,” *Phys. Lett.* **B283** (1992) 145–150.
- [27] J. D. Bjorken, “Highly Relativistic Nucleus-Nucleus Collisions: The Central Rapidity Region,” *Phys. Rev.* **D27** (1983) 140–151.

- [28] G. S. Denicol, T. Koide, and D. H. Rischke, “Dissipative relativistic fluid dynamics: a new way to derive the equations of motion from kinetic theory,” arXiv:1004.5013 [nucl-th].
- [29] A. El, Z. Xu, and C. Greiner, “Third-order relativistic dissipative hydrodynamics,” *Phys. Rev.* **C81** (2010) 041901, arXiv:0907.4500 [hep-ph].
- [30] B. Schenke and M. Strickland, “Photon production from an anisotropic quark-gluon plasma,” *Phys. Rev.* **D76** (2007) 025023, arXiv:hep-ph/0611332.
- [31] M. Martinez and M. Strickland, “Suppression of forward dilepton production from an anisotropic quark-gluon plasma,” arXiv:0808.3969 [hep-ph].
- [32] A. Dumitru, Y. Guo, and M. Strickland, “The heavy-quark potential in an anisotropic (viscous) plasma,” *Phys. Lett.* **B662** (2008) 37–42, arXiv:0711.4722 [hep-ph].
- [33] A. Dumitru, Y. Guo, A. Mocsy, and M. Strickland, “Quarkonium states in an anisotropic QCD plasma,” arXiv:0901.1998 [hep-ph].
- [34] A. Dumitru, Y. Guo, and M. Strickland, “The imaginary part of the static gluon propagator in an anisotropic (viscous) QCD plasma,” *Phys. Rev.* **D79** (2009) 114003, arXiv:0903.4703 [hep-ph].
- [35] A. El, A. Muronga, Z. Xu, and C. Greiner, “A relativistic dissipative hydrodynamic description for systems including particle number changing processes,” arXiv:1007.0705 [nucl-th].
- [36] W. Florkowski and R. Ryblewski, “Highly-anisotropic and strongly-dissipative hydrodynamics for early stages of relativistic heavy-ion collisions,” arXiv:1007.0130 [nucl-th].